



## Performance and purification mechanism of the mullite/SiC composite filter tube membrane

Zhangfu Yuan<sup>1</sup>, Lu Mei<sup>1</sup>, Xuan Peng<sup>1</sup>, Bingsheng Xu<sup>2</sup>, Yuantao Shi<sup>1</sup>, Hongxin Zhao<sup>1,3,\*</sup>

<sup>1</sup>Collaborative Innovation Center of Steel Technology, University of Science and Technology Beijing, 30 Xueyuan Road, Beijing 100083, China

<sup>2</sup>Research Branch of Resource and Environment, China National Institute of Standardization, Beijing 100191, China

<sup>3</sup>National Engineering Research Center of Green Recycling for Strategic Metal Resources, Institute of Process Engineering, Chinese Academy of Sciences, Beijing 100190, China

Received 7 October 2022; Received in revised form 18 January 2023; Accepted 12 February 2023

### Abstract

Asymmetric composite tubular membranes were prepared with SiC as the support body and mullite as the membrane layer. The asymmetric mullite/SiC composite filter tube membranes were characterized by different analytic techniques. The mullite membrane was prepared as a layer on the SiC support with a thickness of about 175  $\mu\text{m}$ , pore size of about 1–10  $\mu\text{m}$  and porosity of 9.9%. The SiC support tube had a pore size of about 20–150  $\mu\text{m}$  and porosity of 19.0%. After 360 days of high-temperature flue gas filtration, the most available pore size of the mullite/SiC composite filter tube membrane reduces from 45.2 to 36.4  $\mu\text{m}$  (the reduction rate of about 19.4%). Analysis of the dust collected by back-blowing revealed that the dust particle size range was between 0.1–100  $\mu\text{m}$  and about 50% of the dust particles were below 2.5  $\mu\text{m}$  in size. The average capture rate of dust can reach 98.4%, indicating that the asymmetric mullite/SiC composite filter tube membrane has excellent filtration performance for the dust below PM<sub>2.5</sub> in the high-temperature complex flue gas.

**Keywords:** SiC support, mullite membrane, composite filter tube membrane, high temperature flue gas

### I. Introduction

Particulate matter (PM) pollution is harmful to human health, especially PM<sub>2.5</sub> particles (having aerodynamic diameter  $\leq 10 \mu\text{m}$ ), which can easily penetrate into human lungs and bronchi and cause diseases of the respiratory system, cardiopulmonary system and other body systems [1,2].

PM pollutants mainly originate from the high-temperature flue gas emitted from industrial furnaces in energy industry, metallurgy, machinery, chemical industry and cement industry [3–6]. In order to relieve the pressure on the environment and achieve sustainable green development, these high-temperature gases need to be purified and treated to reduce industrial PM. Direct filtration of high-temperature flue gas is considered a key technology for effective PM pollution reduction. Nowadays, many technologies have been used to

purify high-temperature flue gas, such as cyclone dust removal technology, electrostatic dust removal technology, high-performance barrier filters etc. [7–9]. However, these technologies have some problems, such as poor filtration effect for dust with particles smaller than 7  $\mu\text{m}$  and cannot work under high-temperature flue gas environment for a long time.

In recent years, porous ceramic filtration membranes have caused a wide research boom in the high-temperature flue gas treatment industry because of their high-temperature resistance, corrosion resistance, high filtration efficiency, low cost, no secondary pollution and long life [10–12]. Ding *et al.* prepared mullite bonded SiC porous complex ceramics by using  $\alpha$ -SiC and  $\alpha$ -Al<sub>2</sub>O<sub>3</sub> as raw materials and graphite as the pore-former after high-temperature sintering in air. The results showed that porous ceramics with porosity ranging from 38% to 56.6% could be produced by the addition of graphite. The porosity increased with the increase of graphite content and the flexural strength in-

\*Corresponding author: tel: +86 13718113630  
e-mail: hxzhao\_ustb@163.com

creased with the increase of sintering temperature. Thus, when porous ceramics was prepared with 27.9 wt.% of graphite and reaction sintered at 1550 °C, the flexural strength and open porosity of the sample were 24.0 MPa and 43.4%, respectively [13]. Liu *et al.* [14] prepared cordierite-bound SiC porous complex-phase ceramics by in situ reaction sintering at high temperatures under air atmosphere using  $\alpha$ -SiC,  $\alpha$ -Al<sub>2</sub>O<sub>3</sub> and MgO as the main raw materials. The results showed that porous complex-phase ceramics with porosity of 23.9% and flexural strength of 74.5 MPa could be produced after the reaction sintering at 1370 °C for 2 h [14].

Traditional filter tube membrane is a symmetrical structure with excellent chemical stability. Still, its low filtration efficiency, low porosity, high resistance, frequent ash cleaning, poor mechanical strength, poor thermal stability, wide pore size distribution and poor filtration performance cannot meet the requirements of industrial applications [15]. The composite filter tube membrane combines support layer with a larger pore size and membrane layer with a smaller pore size into a multilayer structure with asymmetric pore size distribution [16–19]. The inner layer is a support body with a larger average pore size and it ensures the strength of the filter tube. On the other hand, a separation membrane with a smaller particle size is added on the outer surface of the support body to achieve surface filtration of high-temperature flue gas [15,20]. Some studies have shown that silicon carbide, alumina and mullite ceramics have better thermal shock resistance, corrosion resistance and higher mechanical strength in high-temperature gas filtration and are widely used in high-temperature flue gas purification [21–27]. Yuan *et al.* [28] used a hot-pressing process to obtain tubular corundum microporous ceramic filter membrane with uniform pore size distribution. The result showed an excellent filtration effect and corrosion resistance and could be applied to metallurgical high-temperature flue gas treatment for PM<sub>2.5</sub> deep dust removal and purification. Morozova *et al.* [29] prepared ZrO<sub>2</sub>(Y<sub>2</sub>O<sub>3</sub>)-Al<sub>2</sub>O<sub>3</sub> ceramic filter membrane. The zirconia substrate had 20–47% open porosity and pore sizes in the range of 100–300 nm, whereas pore sizes of the nano-alumina layer deposited on it were in the range of 30–100 nm. These types of composite filter tube membranes are currently used in metallurgical industry to filter metallurgical high-temperature flue gas in order to reduce environmental pollution and achieve sustainable green metallurgy.

In this study mullite/SiC composite filter tube membranes were prepared by isostatic pressing of SiC powder to form a support structure and plasma spraying of mullite to create a membrane structure. The mullite/SiC composite filter tube membrane is a double-layer structure with an asymmetric aperture, which cannot only achieve high-efficiency filtration for the high-temperature flue gas but also ensure the strength of the filter membrane. Morphology, pore size distribution,

porosity and roughness of the mullite/SiC composite filter tube membrane were studied. The most available pore sizes, dust capture rate and dust collected by filtration were analysed before and after using mullite/SiC composite filter tube membranes. These analyses were carried out to explore further the high-temperature flue gas separation mechanism of the mullite/SiC composite filter tube membrane.

## II. Experimental

### 2.1. Materials

Silicon carbide (80 μm, purity >99.9%, Aladdin), mullite (*d*: 10–30 μm, *l*: 100–200 μm, purity >99.5%, Beijing), graphite powder (10–120 μm, pore-former, purity >99.5%, Rohn), sodium carboxymethyl cellulose (dispersant, Na-CMC, purity >98%, Rohn), carboxymethyl cellulose (CMC, purity >99.5%, Rohn), pentaerythrityltetrate (lubricant, source leaf biology) and deionized water were used for preparation of the mullite/SiC composite filter tube membrane.

### 2.2. Preparation process

Preparation process of the mullite/SiC composite filter tube membrane is shown in Fig. 1. Silicon carbide and graphite powder (pore-former) were mixed in a ball mill in the ratio 85 : 15. Then, sodium carboxymethyl cellulose as a dispersant was added (the ratio of Na-CMC to SiC/graphite mixture was 3 : 1) and mixed for 5 h to form a slurry. The slurry was put into the ball forming machine and rotary kiln, and then water-soluble binder, lubricant and deionized water were added. The mud was obtained after 24 h of slurry aging within a vacuum mud-making machine. The aged slurry was poured into a mould and the SiC microporous ceramic support embryo (with a length of 1500 mm, outer diameter of 70 mm and a wall thickness of 9 mm) was produced by isostatic moulding. The SiC microporous ceramic support embryos were dried in an infrared drying oven at a temperature of 100 °C for 9 h. The dried embryos were put into the shuttle furnace and fired, the first at a heating rate of 5 °C/min to 750 °C for 2 h and then at a rate of 10 °C/min to 1300 °C for 11 h to obtain the porous ceramic support body. Mullite, water-soluble binder and deionized water were mixed, put into the ball mill for 10 h and then left for 10 h to obtain mullite slurry. After that, the mullite slurry was granulated by YC-015 spray dryer and then it was kept at 1000 °C for 30 min. Finally, a layer of mullite slurry was plasma sprayed on the outer surface of the SiC microporous ceramic support body to form the mullite/SiC composite filter tube membrane. The plasma spraying experimental parameters are shown in Table 1.

### 2.3. Characterization methods

Surface morphology of the mullite/SiC composite filter tube membrane was studied by field emission scanning electron microscopy (FESEM, JSM-7001F).

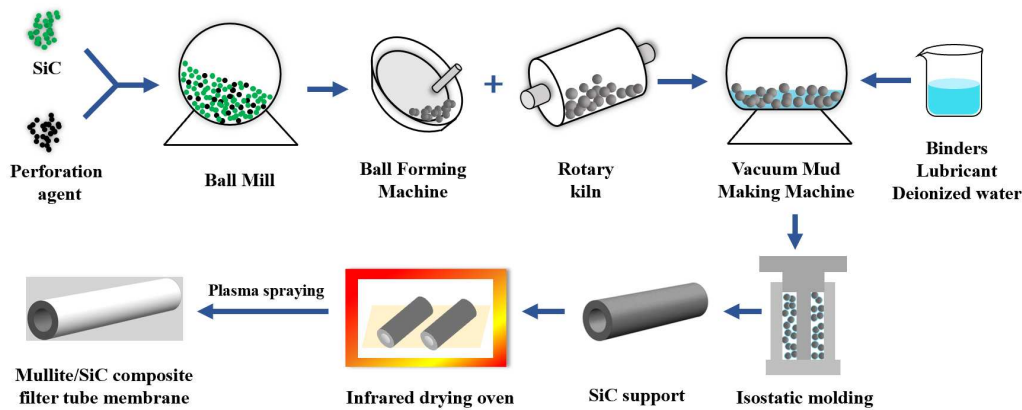


Figure 1. Preparation process of the mullite/SiC composite filter tube membrane

Table 1. Plasma spraying experimental parameters

Power of spray gun	Ar	He	Powder delivery rate	Spray distance	Spraying angle	Rotation speed
35 kW	50 l/min	1.5 l/min	20 g/min	130 mm	60°	30 cm/s

Elemental composition and distribution of the membranes and supports of the mullite/SiC composite filter tube membrane were characterized using an energy spectrometer (EDS, Oxford Instruments, Inca x-max, UK). Crystal structure was detected by X-ray diffraction (XRD, D8 Advance, Bruker, Germany). Phase composition was determined by X-ray photoelectron spectroscopy (XPS, AXIS ULTRADLD). Pore size and distribution of the mullite membrane before and after use were determined using an automated mercury-pressure method (Autopore IV 9500). The membrane surface roughness was measured using an OLS4100 laser confocal scanning microscope. Laser particle size analysis was used to measure the particle size of the collected flue dust.

### III. Results and discussion

#### 3.1. Microstructure and chemical composition

The cross-section of the mullite/SiC composite filter tube membrane was characterized by scanning electron microscope. From Fig. 2a, it can be seen that the mullite/SiC composite filter tube membrane consists of mullite membrane with a thickness of about 175  $\mu\text{m}$

as the upper layer on the SiC support body. Figure 2b shows that the mullite membrane is formed from tightly bonded mullite strips and particles with dimensions of about 100–200  $\mu\text{m}$ . The mutual stacking of mullite particles forms many extended zigzag pores with sizes of about 1–10  $\mu\text{m}$ . The smaller pores of the sprayed layer should show an excellent retention of particulate impurity matter. As shown in Fig. 2c, the SiC support body consists of many coarse grains with a particle size of about 100  $\mu\text{m}$ . There are many irregularly shaped three-dimensional through pores with a pore size of about 20–150  $\mu\text{m}$ . The SiC support body composed of coarse grains forms a strong network structure, which helps improve the strength of the porous ceramics and ensures the strength of the filter membrane.

The chemical composition of the ceramic material has an important influence on its stability. EDS and XRD analyses were used to determine elemental distribution and phase composition of the mullite/SiC composite filter tube membrane (Figs. 3 and 4). As shown in Fig. 3, the mullite/SiC composite filter tube membrane is composed of mullite and SiC, which indicates that both of them have good high temperature stability. The elemental analyses confirm that the mullite/SiC

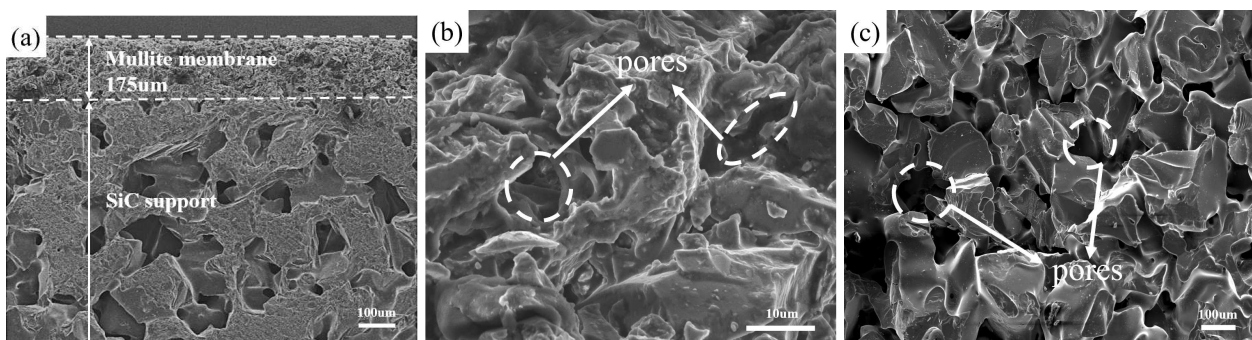


Figure 2. SEM images of the mullite/SiC composite filter tube membrane cross-section: a) full cross-section microstructure, b) mullite membrane and c) SiC support body

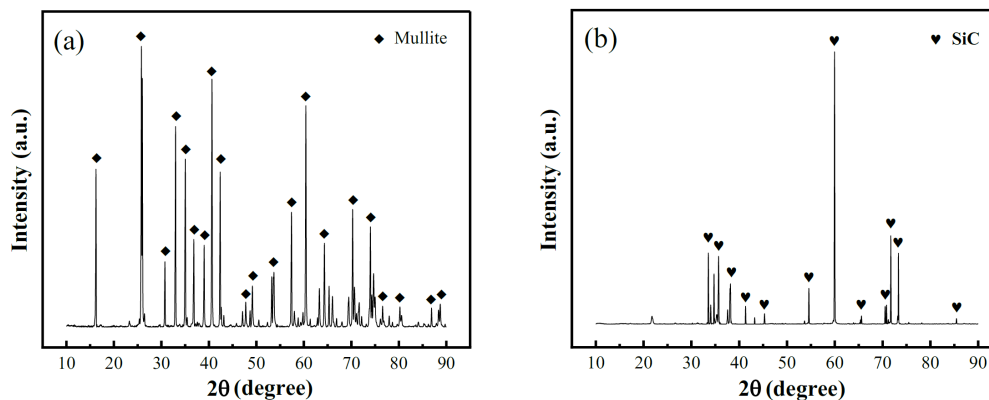


Figure 3. XRD patterns of: a) mullite membrane layer and b) SiC support body

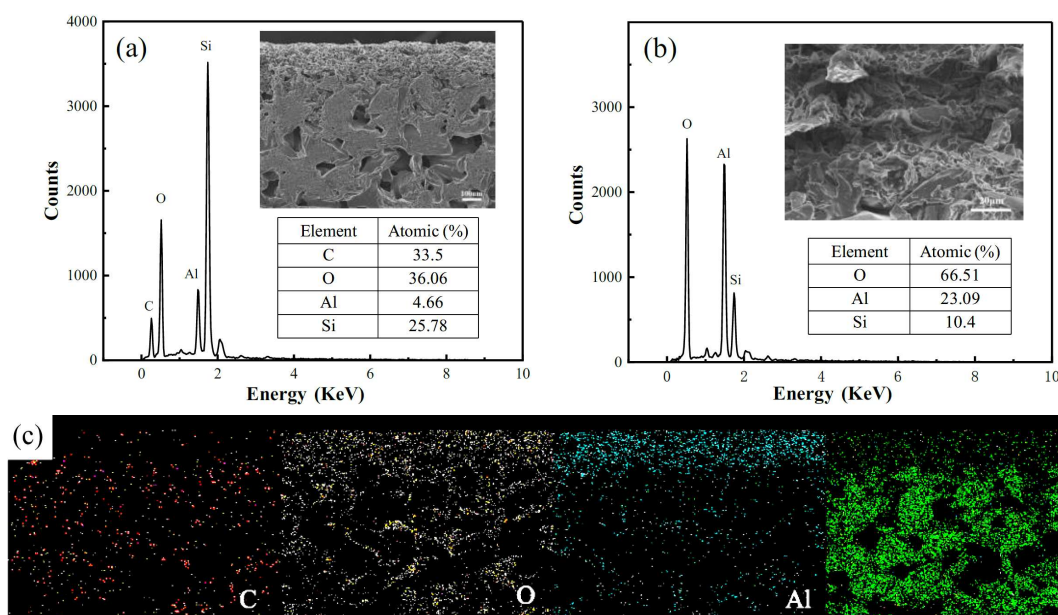


Figure 4. Cross-sectional morphology and EDS analyses of: a) mullite/SiC composite filter tube membrane, b) mullite membrane, and c) elemental distribution of the mullite/SiC composite filter tube membrane

composite filter tube membrane contains 33.5, 36.1, 4.7 and 25.8 at.% of C, O, Al and Si, respectively (Fig. 4a). On the other hand, the mullite membrane contains O, Al and Si, with relative atomic percentages of 66.5%, 23.1% and 10.4%, respectively (Fig. 4b). The distribution of Si and C elements in the support body part of porous SiC ceramic tube membrane is consistent, indicating that the support body of porous silicon carbide ceramic tube membrane is  $\text{Si}_x\text{C}_y$  compound. Figure 4c shows that C and Si elements are mainly distributed in the SiC support, whereas Al is primarily distributed in the mullite membrane. There are apparent boundaries in the distribution area of these three elements. At the same time, the distribution of O is more uniform throughout the cross-section because of the oxygen in the SiC support due to the presence of dispersant, binder and lubricant during the preparation of SiC support.

Figure 5 shows O 1s, Si 2p and Al 2p core energy level spectra of the mullite/SiC composite filter tube membrane. Clear peaks at 531.2 and 532.2 eV are visi-

ble in the O 1s core energy level spectrum (Fig. 5a) originating from aluminosilicate mineral mullite and corresponding to Al–O and Si–O bonds, respectively. The peak at 532.9 eV is due to the C–O bond of hydrocarbons due to the surface adsorption. The Si 2p core energy level spectrum in Fig. 5b shows clear peaks at 102.7 and 103.5 eV, which are attributed to Si–O bonds in the aluminosilicate mineral mullite and the peak at 101.9 eV is due to the contamination during the fabrication process. The Al 2p core energy level spectrum in Fig. 5c shows that the peak at 74.4 eV is attributed to mullite and the peak at 74.6 eV corresponds to Al–O bond, which is also attributed to mullite. The XPS results are consistent with the XRD results.

### 3.2. Porosity and pore size distribution

The pore size distribution and porosity of a composite filter tube membrane significantly influence the gas-solid separation performance [30]. Thus, pore size distribution of the mullite membrane and SiC support were

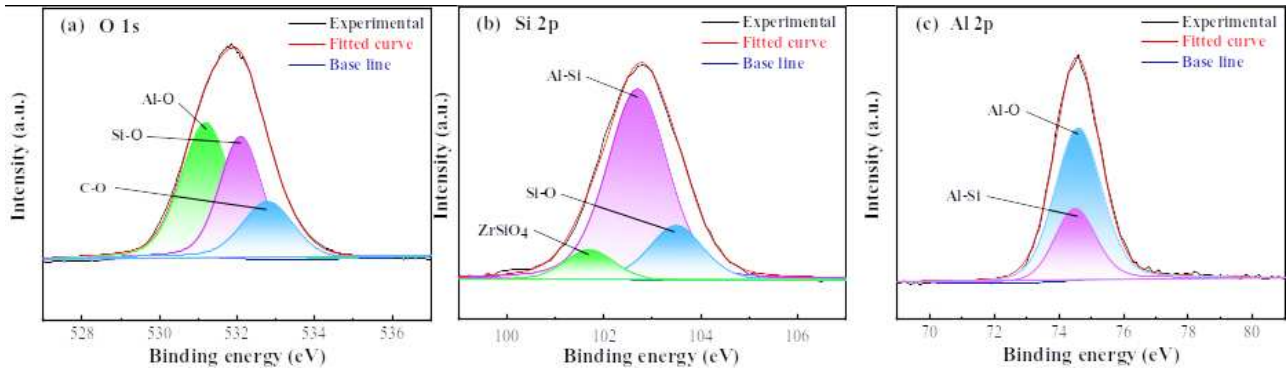


Figure 5. XPS spectrum of the mullite/SiC composite filter tube membrane

measured separately by the binary method and the results are shown in Fig. 6. From Fig. 6a, the pores of the mullite membrane are uniformly distributed, with a pore size of about 1–10  $\mu\text{m}$  and porosity of 9.9%. The smaller pore size indicates that the separation membrane is suitable for micron-level filtration. The bulk particles in the SiC support are uniformly distributed, with a pore size of about 20–150  $\mu\text{m}$  and porosity of 19.0%, and the uniform bulk organization provides sufficient strength for the separation membrane, as shown in Fig. 6b. The pore size measured by the binary method is consistent with the results shown in SEM images. Wang *et al.* [31] prepared porous-foam mullite-bonded SiC-ceramic membranes (MSCMs) with 3D interconnecting-pore network and porosity of the MSCMs was tailored between 69.2% and 84.1%. In comparison, the mullite/SiC composite filter tube membrane prepared in this paper has much smaller porosity.

The pore size distribution of the mullite/SiC composite filter tube membrane at three different locations was measured using the mercury-pressure method to

obtain more accurate results of the pore distribution and its homogeneity analysis. The results are shown in Fig. 7a. Pores of the mullite/SiC composite filter tube membrane at three different locations, upper, middle and lower, have normal and narrow pore size distribution. The vast majority of pores are between 0–100  $\mu\text{m}$ , which is consistent with the SEM results and the most available pore sizes at different locations are similar, about 50  $\mu\text{m}$ . Figure 7b shows the pore size distribution of the mullite/SiC composite filter tube membrane. The results show that the mullite/SiC composite filter tube membrane has similar porosity in the upper, middle and lower parts, i.e. 32.6%, 32.0%, and 29.7%, respectively. Therefore, the mullite/SiC composite filter tube membrane should have good separation performance for gas-solid separation process.

### 3.3. Surface roughness analysis

Many factors affect wear performance of the mullite/SiC composite filter tube membrane during the use. The surface roughness is one of the essential factors and

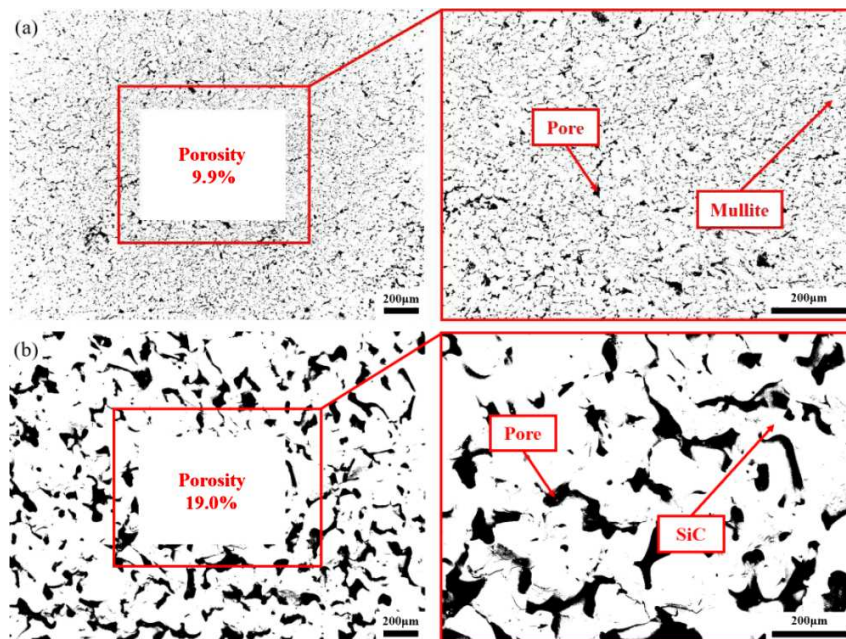


Figure 6. Optical microstructure binary micrographs of the mullite/SiC composite filter tube membrane: a) mullite membrane and b) SiC support body

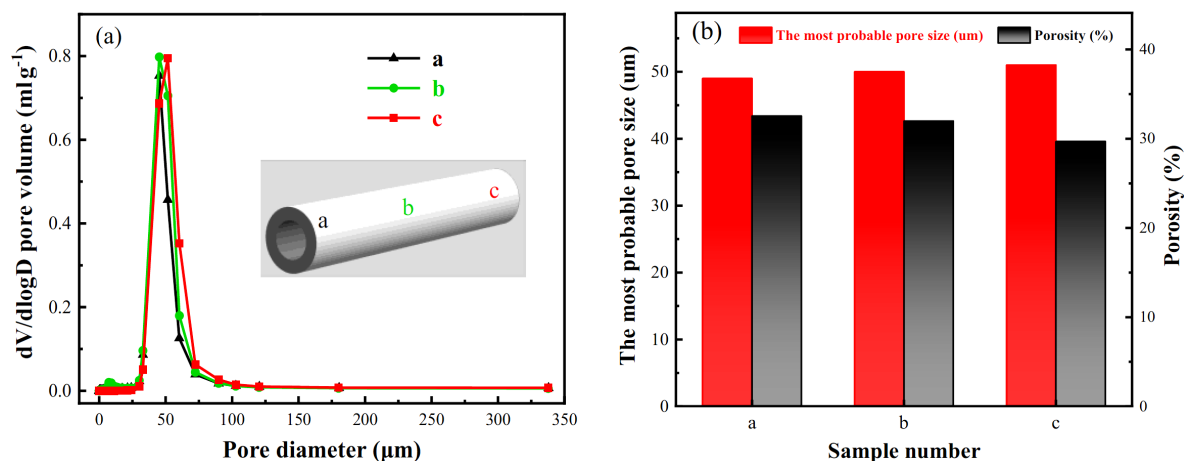


Figure 7. Pore size distribution of the mullite/SiC composite filter tube membrane: a) pore size distribution at different locations and b) porosity and most available pore sizes at different locations

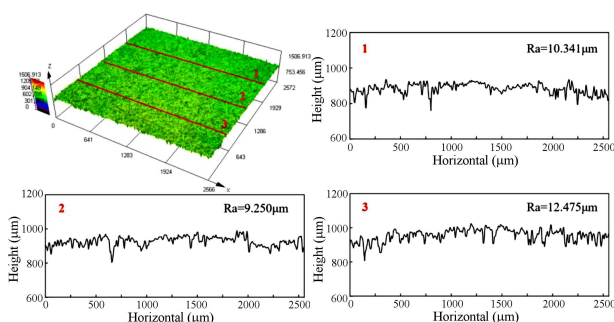


Figure 8. Roughness of the mullite membrane of the mullite/SiC composite filter tube membrane

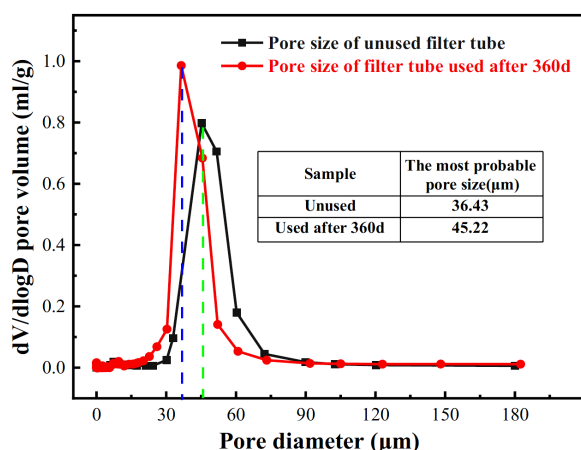


Figure 9. Pore size distribution of the mullite/SiC composite filter tube membrane before and after use

has an important influence on the wettability of impurities in the separation process. Lower surface roughness will reduce the adhesion of impurities [32]. Figure 8 shows the roughness of the mullite layer of the mullite/SiC composite filter tube membrane. The 3D morphology of the mullite layer shows that it has nearly only one colour shade, which indicates that its roughness is minor. The average roughness ( $R_a$ ) was tested at three different locations and corresponding  $R_a$  values were 10.3, 9.25 and 12.5  $\mu\text{m}$ . This confirms that the mul-

lite membrane has uniform surface roughness and fewer defects, so it has good wear performance.

### 3.4. Filtration performances

During the filtration process of metallurgical high-temperature flue gas, the pore plugging rate of a membrane is critical to their separation performance [33]. Thus, the pore size distribution of the mullite/SiC composite filter tube membrane before and after the use was measured using a mercury-pressure instrument (Fig. 9). The pore size distribution of the mullite/SiC composite filter tube membrane before and after the use has normal distribution and the most available pore size was reduced from 45.2 to 36.4  $\mu\text{m}$  after 360 days of filtration. The calculation shows that decrease of the most available pore size of the mullite/SiC composite filter tube membrane is about 19.4%, which is still acceptable from the application point of view.

In the process of flue gas de-dusting, the long-term use of a composite filter tube membrane will deposit a lot of dust on the surface and in its pores and the dust can be collected by reverse blowing. Anhydrous ethanol (analytically pure) was used as the dispersant for the determination of the dust particle size range. Two sets of back-blown dust, A and B, were obtained at the same filtration time and under the same back-blowing conditions at the beginning of the usage period and after 360 days of using. Both samples were probed by using a fully automatic laser particle size analyser (Fig. 10). The particle size range of the samples A and B is basically the same, between 0.1–100  $\mu\text{m}$ , as well as the corresponding particle size distribution. However, there is a slight difference in peak position, which is at 2.42 and 2.74  $\mu\text{m}$  for the samples A and B, respectively. It further shows that the mullite/SiC composite filter tube membrane still has good filtration effect after 360 days of use. Most of the dust particles are distributed in the range of 0.5–7  $\mu\text{m}$  and 16–40  $\mu\text{m}$ . The amount of particles smaller than 2.5  $\mu\text{m}$  is about 50%, indicating that the mullite/SiC composite filter tube membrane has excellent filtration ability for PM2.5 dust particles.

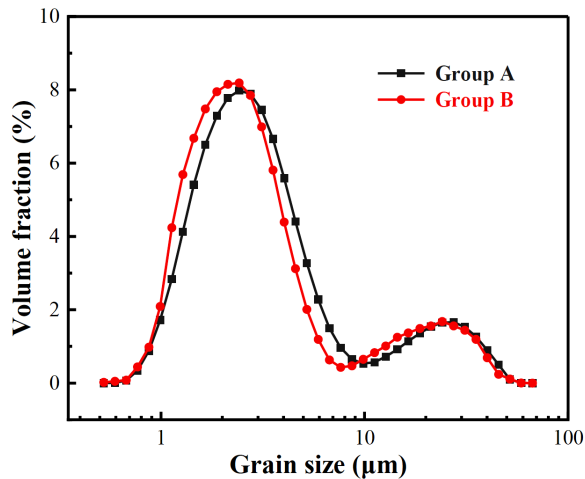


Figure 10. Particle size distribution of the collected fly ash particles

The high-temperature flue gas contains a large amount of dust. When passing through the composite filter membrane, most of the dust is retained due to the dual action of surface filtration and depth filtration of the composite filter membrane. The filtered flue gas contains a tiny amount of fine dust. Therefore, the dust removal efficiency of the composite filter membrane can be determined by the change of dust content in the flue gas before and after filtration. The dust content in the flue gas before and after filtration by the mullite/SiC composite filter tube membrane was measured using a 3012H automatic soot/gas tester. The results of eight tests are shown in Fig. 11. The dust content of high-temperature flue gas is in the range of 320–375 mg/Nm<sup>3</sup>. After filtration by the mullite/SiC composite filtering tube membrane, dust content of the flue gas at the outlet is less than 7 mg/Nm<sup>3</sup> and the minimum can reach 1.37 mg/Nm<sup>3</sup>. The removal efficiency is 98.4% on average, and the maximum removal efficiency can reach 99.6%. Shin *et al.* [34] prepared porous ceramic filter with mullite whiskers by using replica template method and MoO<sub>3</sub> catalyst. The filtering perfor-

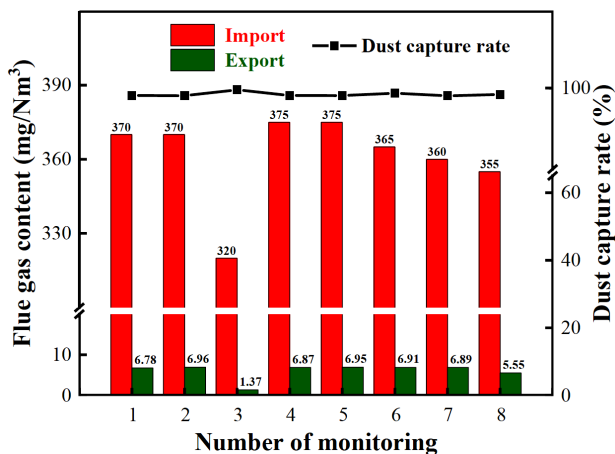


Figure 11. Dust content of inlet and outlet flue gas and dust capture rate

mance gradually improved over filtering time to 86.4% for PM<sub>2.5</sub> and 93.0% for PM<sub>10</sub>. Wang *et al.* [31] prepared porous-foam mullite-bonded SiC-ceramic membranes (MSCMs) with 3D interconnecting-pore network, and the filtration efficiency of PM was recorded at 70.2%, 90.1% and 94.6% for PM<sub>0.3</sub>, PM<sub>2.5</sub> and PM<sub>10</sub>, respectively. In comparison, the mullite/SiC composite filter tube membrane prepared in this paper has better filtration efficiency.

### 3.5. Filtration mechanism

The particle size of flue gas dust is in the range of 1–100 μm, so the separation of dust in this study is a typical microfiltration process, where the separation of components of different particle size ranges is achieved through pressure and concentration differences between the two sides of the membrane. The mechanism of flue gas dust retention depends on the properties (physical and chemical) of the mullite/SiC composite filter tube membrane and the interaction between the mullite membrane and the dust particles. Flue gas is blown in from the outer wall of the mullite/SiC composite filter tube membrane under the atmosphere of NO and O<sub>2</sub>. When the pore size of the mullite membrane is smaller than the size of dust particles in flue gas, the dust particles are blocked from entering or passing through the mullite membrane, and the larger dust particles are directly isolated outside the mullite membrane layer. This separation mechanism is called surface filtration or sieve filtration mechanism. Suppose the pore size of the mullite membrane is larger than the size of impurity particles in the flue gas. In that case, the dust particles can enter the mullite membrane and the SiC support body. The smaller dust particles are “retained” or “adhered” to the pores of the mullite membrane and the SiC support body under the effect of inertial impulse and diffusion. This separation mechanism is called depth filtration. The gases such as N<sub>2</sub>, H<sub>2</sub>O, CO<sub>2</sub>, etc. are discharged from the tube and can be recycled or directly discharged into the atmosphere. After repeated use, the mullite/SiC composite filter tube membrane can be cleaned by reverse blowing, and the collected fly ash can be recycled. The filtration mechanism of the mullite/SiC composite filter tube membrane is shown in Fig. 12.

## IV. Conclusions

In this study mullite/SiC composite filter tube membranes were prepared and their microstructure and functional properties were evaluated. The main conclusions are as follows:

(1) The mullite/SiC composite filter tube membrane consisted of the mullite membrane and the SiC support. The mullite membrane having thickness of 175 μm is formed from tightly bonded mullite strips and particles with dimensions of about 100–200 μm. The SiC support body consisted of many coarse grains with a particle size of about 100 μm.

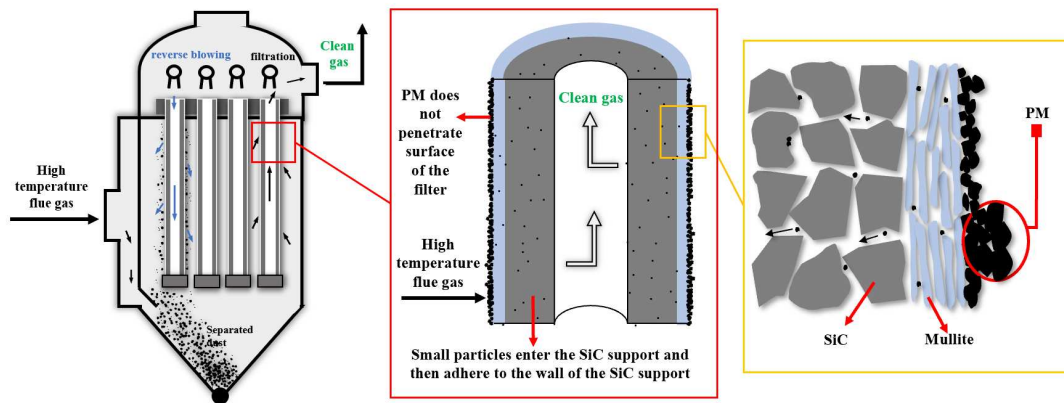


Figure 12. The separation filtration mechanism of the mullite/SiC composite filter tube membrane

(2) There are many zigzag extended pores in the mullite membrane with the size of about 1–10  $\mu\text{m}$  and the total porosity was about 9.9%. In addition, the roughness of the mullite membrane surface is negligible confirmed by similar Ra values at three different locations (i.e. 10.34, 9.25 and 12.48  $\mu\text{m}$ ). There were many irregularly shaped three-dimensional interconnected pores in the cross-section of the SiC support body. The size and porosity of the pores were about 20–150  $\mu\text{m}$  and 19.0%, respectively, and the pore distribution was uniform.

(3) The performance of the mullite/SiC composite filter tube membrane was evaluated. After 360 days of use, the most available pore size of SiC porous ceramic tube reduced from 45.2 to 36.4  $\mu\text{m}$ , which makes the reduction of about 19.4%. The particle size range of the dust collected by reverse blowing was distributed between 0.1–100  $\mu\text{m}$ . Most of them were distributed below 10  $\mu\text{m}$ , and the particles smaller than 2.5  $\mu\text{m}$  accounted for about 50%. After filtration by the mullite/SiC composite filter tube membrane, the removal efficiency was 98.4% on average and the maximum removal efficiency could reach 99.6%, which indicated that the mullite/SiC composite filter tube membrane had a high specific filtration capacity for dust particles.

**Acknowledgements:** This work was supported by the Strategic Priority Research Program of the Chinese Academy of Sciences (Grant No. XDC04010100), President Fund of China Institute of Standardization (542022Y-9371), National Key R&D Program of China (No. 2018YFC1900500), the Natural Science Foundation of China (No. 51974022), the National High Technology Research and Development Program 863 (No. 2013AA065105), and Fundamental Research Funds for the Central Universities (No. FRF-MP-20-17).

## References

1. H. Liu, S. Zhang, L. Liu, J. Yu, B. Ding, "A fluffy dual-network structured nanofiber/net filter enables high-efficiency air filtration", *Adv. Funct. Mater.*, **29** [39] (2019) 1904108.
2. Y. Shi, T. Matsunaga, Y. Yamaguchi, Z. Li, X. Gu, X.

- Chen, "Long-term trends and spatial patterns of satellite-retrieved PM<sub>2.5</sub> concentrations in South and Southeast Asia from 1999 to 2014", *Sci. Total Environ.*, **615** (2018) 177–186.
3. Q. Zhang, Y. Wang, W. Zhang, J. Xu, "Energy and resource conservation and air pollution abatement in China's iron and steel industry", *Resour. Conserv. Recy.*, **147** (2019) 67–84.
4. G. Izydorczyk, K. Mikula, D. Skrzypczak, K. Moustakas, A. Witek-Krowiak, K. Chojnacka, "Potential environmental pollution from copper metallurgy and methods of management", *Environ. Res.*, **197** (2021) 111050.
5. P. Fang, Z. Tang, X. Xiao, J. Huang, X. Chen, P. Zhong, Z. Tang, C. Cen, "Using sewage sludge as a flue gas denitration agent for the cement industry: Factor assessment and feasibility", *J. Clean Prod.*, **224** (2019) 292–303.
6. J. Zhao, B. Li, X. Wei, "Dry processing technology of exhaust gas emitted by roasting of rare earth concentrates with concentrated sulfuric acid", *J. Clean Prod.*, **327** (2021) 129489.
7. M.T. Kanojiya, N. Mandavgade, V. Kalbande, C. Padole, "Design and fabrication of cyclone dust collector for industrial application", *Mater. Today Proc.*, **49** (2022) 378–382.
8. Y.D. Hsu, H.M. Chein, T.M. Chen, C.J. Tsai, "Axial flow cyclone for segregation and collection of ultrafine particles: Theoretical and experimental study", *Environ. Sci. Technol.*, **39** [5] (2005) 1299–1308.
9. B. Xie, S. Li, H. Jin, S. Hu, F. Wang, F. Zhou, "Analysis of the performance of a novel dust collector combining cyclone separator and cartridge filter", *Powder Technol.*, **339** (2018) 695–701.
10. Z. Zhu, J. Xiao, W. He, T. Wang, Z. Wei, Y. Dong, "A phase-inversion casting process for preparation of tubular porous alumina ceramic membranes", *J. Eur. Ceram. Soc.*, **35** [11] (2015) 3187–3194.
11. P.H. Presumido, L.F. Santos, T. Neuparth, M.M. Santos, M. Feliciano, A. Primo, H. Garcia, M. Đolić, V.J.P. Vilar, "A novel ceramic tubular membrane coated with a continuous graphene-TiO<sub>2</sub> nanocomposite thin-film for CECs mitigation", *Chem. Eng. J.*, **430** (2022) 132639.
12. A. Shishkin, H. Aguedal, G. Goel, J. Peculevica, D. Newport J. Ozolins, "Influence of waste glass in the foaming process of open cell porous ceramic as filtration media for industrial wastewater", *J. Clean Prod.*, **282** (2021) 124546.

13. S. Ding, S. Zhu, Y.-P. Zeng, D. Jiang, “Fabrication of mullite-bonded porous silicon carbide ceramics by in situ reaction bonding”, *J. Eur. Ceram. Soc.*, **27** [4] (2007) 2095–2102.
14. S. Liu, Y.-P. Zeng, D. Jiang, “Fabrication and characterization of near-net-shape in situ reaction-bonded porous cordierite/SiC ceramics”, *Int. J. Appl. Ceram. Technol.*, **11** [5] (2014) 839–844.
15. F.D. Minatto, P. Milak, A. De Noni Jr., D. Hotza, O.R.K. Montedo, “Multilayered ceramic composites - A review”, *Adv. Appl. Ceram.*, **114**[3](2015) 127–138.
16. S. Benfer, P. Arki, G. Tomandl, “Ceramic membranes for filtration applications - Preparation and characterization”, *Adv. Eng. Mater.*, **6** [7] (2004) 495–500.
17. Z. Ma, Y. Suzuki, “Hierarchical structure control of MgAl<sub>2</sub>O<sub>4</sub> porous ceramics and application to organic polymer filtration membrane”, *J. Am. Ceram. Soc.*, **104** [12] (2021) 6144–6154.
18. T. Konegger, C.-C. Tsai, H. Peterlik, S.E. Creager, R.K. Bordia, “Asymmetric polysilazane-derived ceramic structures with multiscale porosity for membrane applications”, *Micropor. Mesopor. Mater.*, **232** (2016) 196–204.
19. Z.W. Zhu, Z.L. Wei, W.P. Sun, J. Hou, B.H. He, Y.C. Dong, “Cost-effective utilization of mineral-based raw materials for preparation of porous mullite ceramic membranes via in-situ reaction method”, *Appl. Clay Sci.*, **120** (2016) 135–141.
20. F. Han, Z. Zhong, Y. Yang, W. Wei, F. Zhang, W. Xing Y. Fan, “High gas permeability of SiC porous ceramics reinforced by mullite fibers”, *J. Eur. Ceram. Soc.*, **36** [16] (2016) 3909–3917.
21. Y. Yoshino, T. Suzuki, B.N. Nair, H. Taguchi, N. Itoh, “Development of tubular substrates, silica based membranes and membrane modules for hydrogen separation at high temperature”, *J. Membrane Sci.*, **267** [1-2] (2005) 8–17.
22. M. Fukushima, Y. Zhou, H. Miyazaki, Y.I. Yoshizawa, K. Hirao, Y. Iwamoto, S. Yamazaki T. Nagano, “Microstructural characterization of porous silicon carbide membrane support with and without alumina additive”, *J. Am. Ceram. Soc.*, **89** [5] (2006) 1523–1529.
23. J. Caro, P. Noack, M. Kölsch, “Chemically modified ceramic membranes”, *Micropor. Mesopor. Mater.*, **22** [1] (1998) 321–332.
24. B. Elyassi, M. Sahimi, T.T. Tsotsis, “Silicon carbide membranes for gas separation applications”, *J. Membrane Sci.*, **288** [1-2] (2007) 290–297.
25. G. Xomeritakis, C.M. Braunbarth, B. Smarsly, N. Liu, R. Köhn, Z. Klipowicz, C.J. Brinker, “Aerosol-assisted deposition of surfactant-templated mesoporous silica membranes on porous ceramic supports”, *Micropor. Mesopor. Mater.*, **66** [1] (2003) 91–101.
26. K.A. DeFriend, M.R. Wiesner, A.R. Barron, “Alumina and aluminate ultrafiltration membranes derived from alumina nanoparticles”, *J. Membrane Sci.*, **224** [1-2] (2003) 11–28.
27. Q.K. Lu, X.F. Dong, Z.W. Zhu, Y.C. Dong, “Environment-oriented low-cost porous mullite ceramic membrane supports fabricated from coal gangue and bauxite”, *J. Hazard Mater.*, **273** (2014) 136–145.
28. K. Jiao, X. Yu, Z. Yuan, Y. Zhang, J. Liu, “Enhanced filtration performance of Al<sub>2</sub>O<sub>3</sub>-SiC porous ceramic composite tube depending on microstructure and surface properties”, *Desalin. Water Treat.*, **150** (2019) 99–104.
29. L.V. Morozova, M.V. Kalinina, T.V. Khamova, E.A. Vasil’eva, O.A. Shilova, “Porous ceramics based on the ZrO<sub>2</sub>(Y<sub>2</sub>O<sub>3</sub>)-Al<sub>2</sub>O<sub>3</sub> system for filtration membranes”, *Glass Phys. Cnem.*, **42** [4] (2016) 408–413.
30. Z. Zhu, Y. Cao, X. Dong, X. Meng, Y. Zhao, Z. Ding, Z. Wei, “Cost-effective porous ceramic tubes fabricated through a phase inversion/casting process using calcined bauxite”, *Int. J. Appl. Ceram. Technol.*, **15** [6] (2018) 1567–1576.
31. F. Wang, S. Hao, B. Dong, N. Ke, N.Z. Khan, L. Hao, L. Yin, X. Xu, S. Agathopoulos, “Porous-foam mullite-bonded SiC-ceramic membranes for high-efficiency high-temperature particulate matter capture”, *J. Alloys Compd.*, **893** (2022) 162231.
32. W. Zhang, S. Yamashita, T. Kumazawa, F. Ozeki, H. Hyuga, H. Kita, “Influence of surface roughness parameters and surface morphology on friction performance of ceramics”, *J. Ceram. Soc. Jpn.*, **127** [11] (2019) 837–842.
33. Z. Deng, C.H. Nicolas, M.O. Daramola, J. Sublet, T. Schiestel, A.J. Burger, Y. Guo, A. Giroir-Fendler, M. Perattus, “Nanocomposite MFI-alumina hollow fibre membranes prepared via pore-plugging synthesis: Influence of the porous structure of hollow fibres on the gas/vapour separation performance”, *J. Membrane Sci.*, **364** [1] (2010) 1–8.
34. C. Shin, D.-K. Lee, S.-H. Oh, J.-H. Choi, K.-T. Hwang, K.-S. Han, J.-H. Kim, “Filtering performance of ceramic filter with mullite whisker for non-exhaust particulate matter from transportation”, *J. Mater. Res. Technol.*, **23** (2023) 165–171.